## New Constraints on Axionlike Particles with the NEON Detector at a Nuclear Reactor

Byung Ju Park, <sup>1,2</sup> Jae Jin Choi, <sup>3,2</sup> Eunju Jeon, <sup>2,1</sup> Jinyu Kim, <sup>4</sup> Kyungwon Kim, <sup>2</sup> Sung Hyun Kim, <sup>2</sup> Sun Kee Kim, <sup>3</sup> Yeongduk Kim, <sup>2,1</sup> Young Ju Ko, <sup>2,‡</sup> Byoung-Cheol Koh, <sup>5</sup> Chang Hyon Ha, <sup>5</sup> Seo Hyun Lee, <sup>1,2</sup> In Soo Lee, <sup>2,\*</sup> Hyunseok Lee, <sup>1,2</sup> Hyun Su Lee, <sup>2,1,†</sup> Jaison Lee, <sup>2</sup> Yoomin Oh, <sup>2</sup>

(NEON Collaboration)

Doojin Kim<sup>®</sup>, <sup>6,7</sup> Gordan Krnjaic<sup>®</sup>, <sup>8,9,10</sup> and Jacopo Nava<sup>®</sup> <sup>11,12</sup>

<sup>1</sup>IBS School, University of Science and Technology (UST), Deajeon 34113, Republic of Korea

<sup>2</sup>Center for Underground Physics, Institute for Basic Science (IBS), Daejeon 34126, Republic of Korea

<sup>3</sup>Department of Physics and Astronomy, Seoul National University, Seoul 08826, Republic of Korea

<sup>4</sup>HANARO Utilization Division, Korea Atomic Energy Research Institute (KAERI), Deajeon 34057, Republic of Korea

<sup>5</sup>Department of Physics, Chung-Ang University, Seoul 06973, Republic of Korea

<sup>6</sup>Department of Physics, University of South Dakota, Vermillion, South Dakota 57069, USA

<sup>7</sup>Mitchell Institute for Fundamental Physics and Astronomy, Department of Physics and Astronomy, Texas A&M University, College Station, Texas 77845, USA

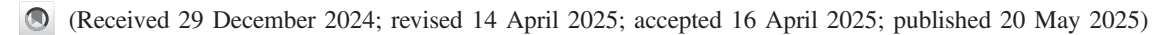
<sup>8</sup>Theoretical Physics Division, Fermi National Accelerator Laboratory, Batavia, Illinois 60510, USA

<sup>9</sup>Department of Astronomy & Astrophysics, University of Chicago, Chicago, Illinois 60637, USA

<sup>10</sup>Kavli Institute for Cosmological Physics, University of Chicago, Chicago, Illinois 60637, USA

<sup>11</sup>Dipartimento di Fisica e Astronomia, Università di Bologna, via Irnerio 46, 40126, Bologna, Italy

<sup>12</sup>INFN, Sezione di Bologna, viale Berti Pichat 6/2, 40127, Bologna, Italy



We report new constraints on axionlike particles (ALPs) using data from the NEON experiment, which features 16.7 kg of NaI(Tl) target located 23.7 m from a 2.8 GW thermal power nuclear reactor. Analyzing a total exposure of 3063 kg · day, with 1596 kg · day during reactor-on and 1467 kg · day during reactor-off periods, we compared energy spectra to search for ALP-induced signals. No significant signal was observed, enabling us to set exclusion limits at the 95% confidence level. These limits probe previously unexplored regions of the ALP parameter space, particularly for axion masses ( $m_a$ ) near 1 MeV/ $c^2$ . For ALP-photon coupling ( $g_{a\gamma}$ ), limits reach as low as  $6.24 \times 10^{-6}$  GeV<sup>-1</sup> at  $m_a = 3.0$  MeV/ $c^2$ , while for ALP-electron coupling ( $g_{ae}$ ), limits reach 4.95 × 10<sup>-8</sup> at  $m_a = 1.02$  MeV/ $c^2$ . This Letter demonstrates the potential for future reactor experiments to probe unexplored ALP parameter space.

DOI: 10.1103/PhysRevLett.134.201002

Axions were first proposed in 1977 by Peccei and Quinn [1] to address the strong *CP* problem in quantum chromodynamics (QCD) [2,3]. Because of their extremely light mass and weak interactions with ordinary matter, axions are considered promising candidates for dark matter [4–8].

Published by the American Physical Society under the terms of the Creative Commons Attribution 4.0 International license. Further distribution of this work must maintain attribution to the author(s) and the published article's title, journal citation, and DOI. Funded by SCOAP<sup>3</sup>. Despite numerous experimental searches, axions have not yet been detected [9–12]. The concept has since been extended to include axionlike particles (ALPs) in various models [13,14]. While ALPs share many properties with axions, making them viable dark matter candidates, they are not necessarily tied to solving the strong *CP* problem [15]. ALPs can span a wide range of masses and coupling constants, leading to diverse phenomenological implications in astrophysical and laboratory contexts [14].

ALPs interact with standard model particles, particularly photons and electrons, motivating extensive experimental searches [12]. Light ALPs (axion mass,  $m_a < 100 \text{ keV/c}^2$ ) are typically investigated using solar helioscopes, haloscopes, or photon regeneration experiments [16]. In contrast, heavy ALPs ( $m_a > 100 \text{ keV/c}^2$ ) are probed using colliders or beam dump experiments [17–19].

<sup>\*</sup>Contact author: islee@ibs.re.kr

†Contact author: hyunsulee@ibs.re.kr

<sup>\*</sup>Present address: Department of Physics, Jeju National University, Jeju 63243, Korea.

Astrophysical observations provide complementary constraints on the ALP parameter space [20,21].

A particularly intriguing region of ALP parameter space, known as the "cosmological triangle" [22,23], spans masses between 0.3 and 8 MeV/c² with an axion-photon coupling constant  $(g_{a\gamma})$  ranging from  $1.8 \times 10^{-6}$  to  $5 \times 10^{-5}$  GeV<sup>-1</sup>. This region remains largely unexplored by both direct searches and astrophysical bounds. Although model-dependent cosmological constraints [24] restrict this region, they can be evaded under nonstandard cosmological scenarios [25,26].

Recent supernova-based constraints from Ref. [27] suggest coverage of this region; however, these results depend on specific assumptions about the muonic supernova core and the Garching supernova model [28,29]. Notably, ALP production and the corresponding constraints depend strongly on supernova mechanisms and ALP model parameters. Recent studies suggest that in certain regimes, loop-induced ALP-photon interactions may dominate over muonic processes, potentially altering the derived limits [30].

Growing interest in this region [23] has driven studies exploring the potential for direct ALP searches with significantly less model dependence. These include short-baseline reactor experiments [31,32], the accelerator-based coherent CAPTAIN-Mills (CCM) experiment with a 10-ton liquid argon target [33], DUNE-like future neutrino experiments with a 50-ton liquid or gaseous argon target [22], and a 2-kton liquid scintillator with an intense proton beam underground [34].

Nuclear reactors are the most intense sources of photons with energies up to a few MeV. Since ALPs can be produced via photon-induced scattering [14], reactors offer a promising avenue for ALP searches in the MeV/c² mass range. However, only a few reactor-based ALP searches have been conducted [35,36]. In reactor-based ALP searches, data collected during reactor operation (reactor-on data) can be compared to data collected when the reactor is inactive (reactor-off data) to constrain potential ALP signals. ALPs are primarily produced via Primakoff or Compton-like processes and detected through decay or scattering channels.

In this Letter, we present a direct search for ALPs using the NEON (neutrino elastic scattering observation with NaI) experiment [37]. Leveraging the intense ALP production from the reactor core, the NEON experiment begins to probe the unexplored cosmological triangle in a laboratory-based experiment. For axion-electron couplings, this Letter investigates previously uncharted parameter space for axion masses between 300 keV/ $c^2$  and 1 MeV/ $c^2$ .

The NEON experiment is designed to detect coherent elastic neutrino-nucleus scattering (CE $\nu$ NS) using reactor electron antineutrinos [37]. The detector is located in the tendon gallery of the 2.8 GW Hanbit nuclear power reactor, 23.7  $\pm$  0.3 m from the center of the reactor core. After an

engineering run in 2021 [37], the detector encapsulation was upgraded to enhance long-term operational stability [38].

The NEON detector consists of four 8-in. and two 4-in. long, 3-in. diameter NaI(Tl) crystals, with a total mass of 16.7 kg. The six NaI(Tl) modules are submerged in 800 l of liquid scintillator. This liquid scintillator helps identify and reduce radioactive backgrounds affecting the NaI(Tl) crystals [39]. To further reduce external radiation background, the liquid scintillator is surrounded by shielding made of lead, borated polyethylene, and high-density polyethylene [37].

Each NaI(Tl) crystal is coupled to two photomultiplier tubes (PMTs) without quartz windows, optimizing light collection efficiency [38,40]. The crystal-PMT assemblies are enclosed in a copper casing to ensure structural integrity and prevent exposure to external air or liquid scintillator [38]. Events that satisfy the trigger condition—coincident photoelectrons detected by both of the crystal's PMTs within a 200 ns window—are recorded using 500 MHz flash analog-to-digital converters (FADCs). These events are stored as 8 us waveforms, beginning 2.4 us before the trigger [37,41]. The system records two readouts: a highgain signal from the anode for the 0-60 keV energy range and a low-gain signal from the fifth-stage dynode for the 60-3000 keV range, similar to the setup used in the COSINE-100 experiment [41]. To reject unwanted phosphorescence events from direct muon hits, a 300 ms dead time is applied for energy deposits exceeding approximately 3 MeV.

The data analyzed in this Letter were collected between April 11, 2022 and June 22, 2023, yielding a total live time exposure of 5702 kg · day. Data collection was generally stable, although downtime occurred due to unexpected power outages. To ensure reactor security, the absence of an online connection extended downtime during summer 2022. Despite these challenges, the data acquisition (DAQ) system maintained an average efficiency of approximately 70% throughout the data-taking period.

At the start of physics operations, we collected data while the reactor was operating at full power (reactor-on data) for 120 day. However, an unexpected power outage caused the NEON DAQ system to be offline for 38 day during this period. The reactor was inactive from September 26, 2022, to February 22, 2023, for regular maintenance and fuel replacement, during which reactor-off data were collected for 144 day. After maintenance, the reactor resumed operation on February 22, 2023. To avoid complexities arising from changes in photon and ALP fluxes, data from ramp-down and ramp-up periods were excluded. Once the reactor restarted, it operated stably at full power. Data collected through June 22, 2023, added an additional 117 day of reactor-on exposure.

Various internal and external radiation peaks were used to calibrate the energy scale and resolution, following procedures similar to those adopted in the COSINE-100

experiment [42,43]. Internal and external background peaks include 31 keV from <sup>121</sup>mTe, 39 and 67 keV from <sup>125</sup>I, 49 keV from <sup>210</sup>Pb, 295 keV from <sup>214</sup>Pb, 609 and 1764 keV from <sup>214</sup>Bi, 1461 keV from <sup>40</sup>K, and 2615 keV from <sup>208</sup>Tl. External calibrations were also performed using radioactive sources, yielding peaks at 60 keV from <sup>241</sup>Am and 511 and 1274 keV from <sup>22</sup>Na [37]. It is well known that scintillators like NaI(Tl) crystals exhibit a nonproportional relationship between energy deposition and light output [44]. The nonproportional response model, characterized using the COSINE-100 NaI(Tl) crystals [43], was applied to correct the energy scale used in this analysis.

This analysis focused on events with energies between 3 and 3000 keV. The region below 3 keV was dominated by PMT-induced noise pulses and afterpulses from energetic events such as cosmic muons, and inclusion of this region did not significantly enhance sensitivity to ALP signals. Therefore, we excluded it from the analysis to ensure robustness. Above 3 keV, residual noise events were well rejected using a boosted decision tree (BDT)-based event selection algorithm [45], with no loss of efficiency. Although this analysis was not significantly affected by low-energy noise, the same data quality cuts developed for low-energy analyses—such as CE\(\nu\)NS and low-mass dark matter searches [46]—were applied for consistency. Data quality was monitored by evaluating event rates in the 1-3 keV range after BDT selection. Each 1 h dataset was classified as "good" if its event rate fell within  $3\sigma$  of the mean event rate distribution; otherwise, it was classified as "bad." In total, this analysis utilized 1596 kg · day of reactor-on data and 1467 kg · day of reactor-off data.

Selected events were further categorized as single-hit or multiple-hit events. A multiple-hit event was defined as having accompanying crystal signals with more than four photoelectrons or a liquid scintillator signal exceeding 80 keV within a 150 ns time coincidence window. Events that did not meet these criteria were classified as single-hit samples.

Most background contributions in the NaI(Tl) detectors remain stable over a 1.2 yr data acquisition period [47]. Although the dominant <sup>210</sup>Pb contamination has a half-life of 22.3 yr, its variation during the 1.2 yr data period is negligible. We thus define the effectively time-independent background components as the "continuum background," which includes internal contaminants, surface contamination, and external radiation, with a half-life equal to or greater than that of <sup>210</sup>Pb. In addition to the continuum background, we identified a few time-dependent backgrounds. Short-lived cosmogenic contaminants in the NaI (Tl) crystals, introduced by cosmic ray exposure before installation, were characterized through dedicated analysis [48]. Seasonal variations in <sup>222</sup>Rn levels, with higher levels observed in summer due to temperature changes [49], can affect the time-dependent background. Dust contamination introduced during detector upgrades contained long-lived isotopes, which settled to the bottom of the liquid scintillator, leading to a gradual decrease in the background rate over time.

To account for time-dependent backgrounds, we divided the dataset into seven two-month periods and extracted contributions from <sup>222</sup>Rn and dust, as detailed in the Supplemental Material [50] (see also references [37,38,42,48,49,51–54] therein). This model enables us to characterize the backgrounds observed in reactor-on (a) and reactor-off (b) periods, as exemplified in the detector-6 single-hit data shown in Fig. 1. The remaining background in the reactor-on-minus-off dataset (c) is also modeled. The measured data are well described by the expected backgrounds including time-dependent background components.

Considering the varying event rates across different energy ranges, we employed dynamic energy bins ranging from 57 keV (3–60 keV) to 600 keV (2400–3000 keV). Figure 2 presents the ALP search data from detector-6, based on the reactor-on-minus-off spectra, in which both single-hit and multiple-hit channels are used simultaneously.

Intense photons are generated in the nuclear reactor through nuclear fission, the decay of fission products, capture processes, decay of capture products, and scattering [55], with the photon flux approximated from the FRJ-1 research reactor [56]. We consider a generic model in which an ALP couples to either photons or electrons. For photon coupling, ALPs can be produced through the Primakoff process  $(\gamma + A \rightarrow a + A)$ , where a photon  $(\gamma)$ interacts with a nucleus (N) to produce an axion (a) [57]. Detection occurs through two-photon decay  $(a \rightarrow \gamma \gamma)$  or the inverse Primakoff process, with rates depending on the axion-photon coupling constant  $(g_{ay})$ . For electron coupling, ALPs can occur through the Compton-like process  $(\gamma + e^- \rightarrow a + e^-)$  and be detected through electronpositron pair production  $(a \rightarrow e^-e^+)$ , axioelectric absorption  $(a + e^- + A \rightarrow e^- + A)$ , or inverse Compton-like process  $(a + e^- \rightarrow \gamma + e^-)$ . The rate of these processes depends on the strength of the axion-electron coupling constant  $(g_{ae})$ . To model detector responses, we employ GEANT4-based simulations. Two benchmark ALP signals,  $m_a = 1 \text{ MeV/c}^2$ ,  $g_{a\gamma} = 3 \times 10^{-5} \text{ GeV}^{-1}$  for axion-photon coupling and  $m_a = 10 \text{ keV/c}^2$ ,  $g_{ae} = 8 \times 10^{-6}$  for axionelectron coupling, are compared to the measured spectra in Fig. 2. For ALP-electron couplings, signals typically deposit energy within a single crystal, while ALP-photon interactions can produce high-energy photons that Compton scatter across multiple detectors, leading to multiple-hit events. We do not consider the ALP production through the nuclear deexcitation, as studied by the TEXONO experiment [35]. Further details on ALP signal generation in the NEON detector are provided in Supplemental Material [50] (see also Refs. [31,32,55–62] therein).

Several sources of systematic uncertainty are included in our modeling of the reactor-on-minus-off spectra. These include potential variations in detector responses between

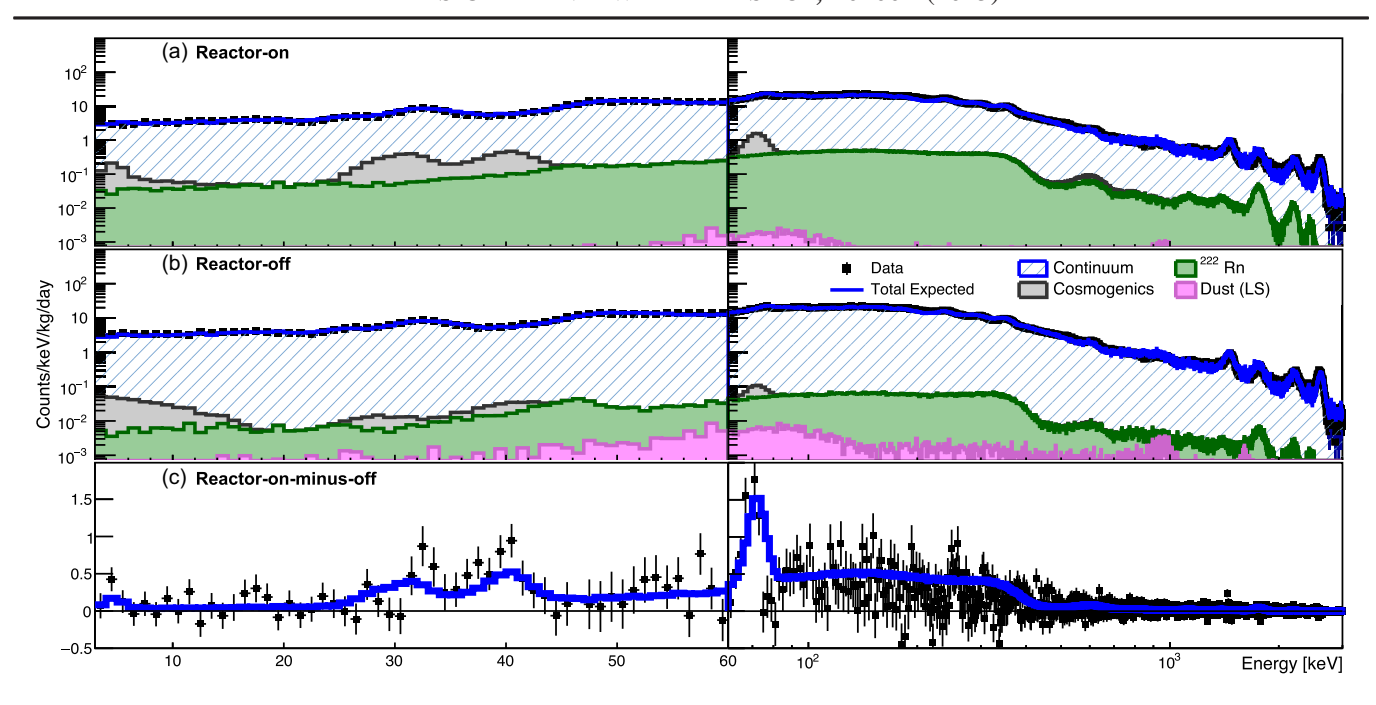


FIG. 1. Single-hit energy spectra of the detector-6 module. The figure shows the normalized energy spectra of single-hit events (black points) in the detector-6 module, compared with the expected background contributions (blue solid lines) for reactor-on data (a), reactor-off data (b), and the reactor-on-minus-off spectrum (c). The expected background includes time-independent continuum components and time-dependent contributions such as cosmogenic activation, <sup>222</sup>Rn in the calibration holes, and <sup>238</sup>U and <sup>232</sup>Th from dust contamination in the liquid scintillator. For the reactor-on-minus-off spectrum (c), only time-dependent components contribute to the background.

the reactor-on and the reactor-off periods. The largest systematic uncertainties are associated with the time-dependent background modeling of <sup>222</sup>Rn variation, as well as uranium and thorium concentrations in the dust.

Additionally, possible contamination of <sup>222</sup>Rn into the liquid scintillator and different locations of the dust also contribute to systematic uncertainties. Figure 2 indicates systematic uncertainty bands for the expected background.

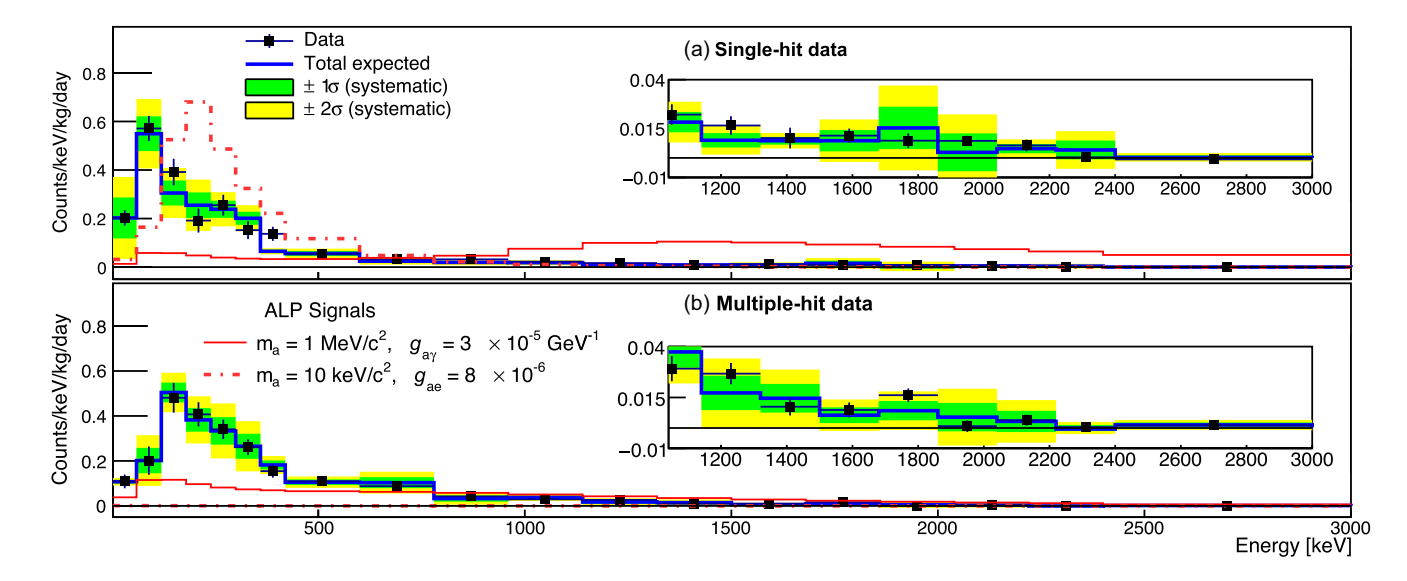


FIG. 2. ALP search data from detector-6 module. This figure presents the reactor-on-minus-off data spectra used for ALP signal searches in the detector-6 module. The data is shown for both single-hit (a) and multiple-hit (b). The data points (black circles) and the expected background spectra (blue solid lines) are derived from the models presented in Fig. 1, but with different bin sizes used for this analysis. The green and yellow bands indicate 68% and 95% confidence level intervals for the background model, respectively. The inset zooms in the high-energy region for better visibility. Two benchmark ALP signals are overlaid for comparison:  $m_a = 10 \text{ keV/c}^2$ ,  $g_{ae} = 8 \times 10^{-6}$  (red dashed line) and  $m_a = 1 \text{ MeV/c}^2$ ,  $g_{a\gamma} = 3 \times 10^{-5}$  GeV<sup>-1</sup> (red solid line).

While the reactor-on-minus-off background rate is allowed to vary by approximately 20% to account for these effects, the resulting impact on the exclusion limit is modest: the sensitivity to the ALP coupling constant changes by less than 3%, as the signal rate scales with the fourth power of the coupling constant. Furthermore, we account for a 10% uncertainty in the reactor photon flux, originating from differences between the FRJ-1 research reactor model and the commercial Hanbin reactor, for which no detailed photon spectrum is publicly available. This 10% variation leads to an additional 2.4% change in the derived axion-photon and axion-electron coupling limits.

The NEON data are fitted for each ALP mass and interaction type. We use various simulated ALP signals to evaluate their potential contributions to the measured energy spectra of the reactor-on-minus-off data (shown in Fig. 2). A  $\chi^2$  fit is applied to the measured spectra (both single-hit and the multiple-hit channels) between 3 and 3000 keV for each ALP signal and various ALP masses. Each crystal and channel is fitted with a crystal-channel specific background model and a crystal-channel correlated ALP signal. The combined fit is achieved by summing the  $\chi^2$  values from the all crystals and channels. No statistically significant excess of events was found for any of the considered ALP signals. The posterior probabilities of the signals are consistent with zero in all cases, and 95% confidence level limits are determined.

Figure 3(a) presents the 95% confidence level exclusion limit derived from NEON data for ALPs coupled solely to photons. This limit is shown in the two-dimensional parameter space of  $m_a - g_{a\gamma}$ . For ALP masses below 20 keV/c<sup>2</sup>, the dominant contribution arises from the scattering process via the inverse Primakoff process. At higher ALP masses, the limit is set by the  $a \rightarrow \gamma \gamma$  decay

process. Since this decay can occur within the 23.7 m flight path, limits are considered for both lower and higher  $g_{a\gamma}$  values. For ALP masses above 3 MeV/c², sensitivity declines due to detector saturation effects and the decreasing reactor photon flux at higher energies. However, signatures of Compton scattering could still allow searches for higher-mass ALPs. In this process, a high-energy photon from the ALP interaction deposits a lower-energy electron or photon within the detectable range. Future improvements, such as reconstructing saturated events—similar to techniques employed in the COSINE-100 experiment for boosted dark matter searches [63]—could enhance sensitivity to higher-mass ALPs.

The exclusion limits shown in Fig. 3(a) extend to previously unexplored regions of ALP parameter space, surpassing existing constraints from beam dump experiments and astrophysical and cosmological limits as adapted from Refs. [75,76]. Notably, this Letter starts to probe the cosmological triangle, a previously unconstrained region between beam dump experiments and astrophysical bounds. A small remaining region of the KSVZ QCD axion model parameter space [74], corresponding to axion masses of a few hundred  $keV/c^2$ , is partially ruled out. The exclusion limit reaches lower  $g_{a\gamma}$  values, down to  $6.24 \times 10^{-6} \text{ GeV}^{-1} \text{ for } \text{m}_a = 3.0 \text{ MeV/c}^2$ . Compared to a recent reactor-based ALP search using CsI(Tl) crystals [36], the NEON experiment significantly improved the lower bound on  $g_{a\gamma}$ , benefiting from a larger exposure and lower background levels in NaI(Tl) crystals. However, the greater distance from the reactor core to the NEON detector results in a reduced upper bound. This Letter provides new experimental constraints from a direct ALP search with reduced model dependence.

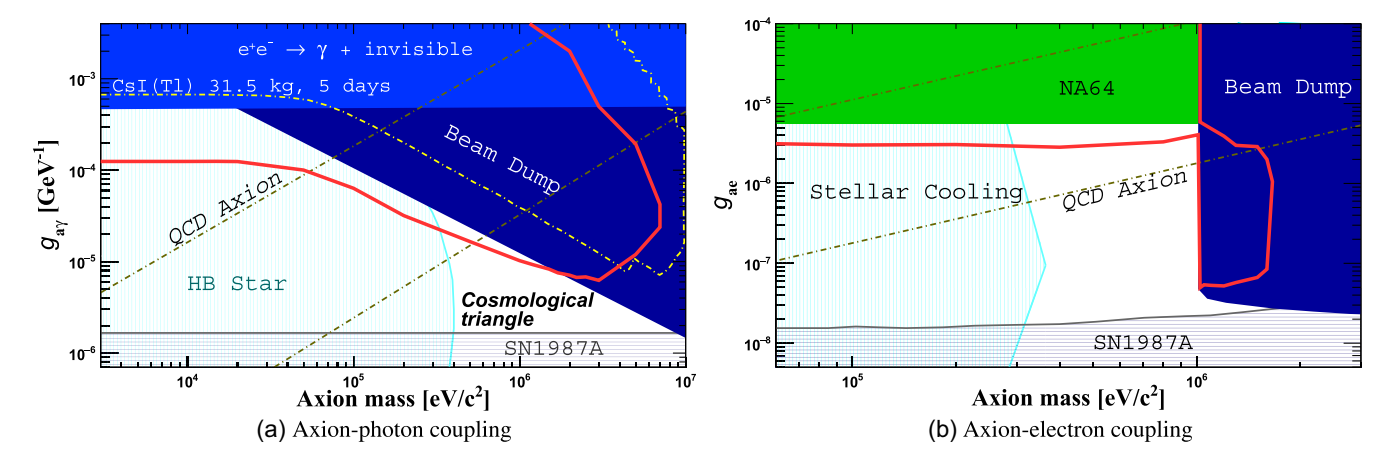


FIG. 3. Exclusion limits of the ALP interactions. The observed 95% confidence level exclusion limit (red solid line) derived from NEON data for the axion photon (a) and the axion electron (b) are compared with limits from beam dump experiments [17,64–67], SN1987A [68–70],  $e^+e^- \rightarrow \gamma$  + invisible states [71], HB stars cooling arguments [25], stellar cooling constraints [72], the NA64 missing energy search [73], and CsI(Tl) exposure in a nuclear reactor [36]. The QCD axion model parameter spaces of the KSVZ [74] and DFSZ(I) [74] benchmark scenarios for the axion-photon coupling and axion-electron coupling, respectively, are indicated by the gray dashed lines.

Figure 3(b) displays the 95% confidence level exclusion limit for ALPs coupled purely to electrons, presented in the  $m_a-g_{ae}$  parameter space. For ALP masses below 1.02 MeV/c², the limit is primarily set by scattering processes via the inverse Compton-like process and axioelectric absorption. For higher ALP masses ( $m_a > 1.02 \text{ MeV/c²}$ ), the limit is dominated by the  $a \rightarrow e^+e^-$  decay process, which has a kinematic threshold of  $m_a > 2m_e = 1.02 \text{ MeV/c²}$  (where  $m_e$  is the electron mass). Similar to the ALP-photon case, limits are considered for both upper and lower bounds due to potential ALP decay during flight.

The NEON data also explore previously examined regions constrained by stellar cooling arguments [20] for axion masses below 300 keV/c<sup>2</sup>, where environmental effects could allow circumvention of these limits [32]. In the mass range of 300 keV/ $c^2$  and 1.02 MeV/ $c^2$ , scattering processes probe coupling values down to  $g_{ae}$  about  $3 \times 10^{-6}$ , which were previously unexplored by direct searches or astrophysical and cosmological considerations. This limit extends into regions predicted by the DFSZ-I QCD axion model [74]. For ALP masses above the kinematic limit for  $a \rightarrow e^+e^-$  (m<sub>a</sub> > 1.02 MeV/c<sup>2</sup>), the NEON data compete with limits from beam dump experiments [65–67]. The exclusion limit reaches lower  $g_{ae}$ values, down to  $4.95 \times 10^{-8}$  for  $m_a = 1.02 \text{ MeV/c}^2$ . The NEON search for axion-electron coupling is currently limited to ALP masses below 1.6 MeV/c<sup>2</sup> due to the 3 MeV dynamic range of the analysis. Similar to the ALPphoton case, reconstructing saturated events above 3 MeV energies could extend the search to higher ALP masses, as demonstrated in Refs. [32,36].

This Letter reports a direct search for axionlike particles using the NEON experiment. Leveraging 16.7 kg of NaI(Tl) crystals located 23.7m from a 2.8 GW thermal power reactor core, NEON has set new exclusion limits for ALPs coupling to photons and electrons. These results probe previously inaccessible regions of ALP parameter space, particularly axion masses around 1 MeV/ $c^2$ , for both axion-photon and axion-electron couplings. Future improvements, such as increased data exposure and advanced reconstruction of saturated events above 3 MeV, will further enhance NEON's sensitivity to ALP searches.

Acknowledgments—We thank the Korea Hydro and Nuclear Power (KHNP) company for the help and support provided by the staff members of the Safety and Engineering Support Team of Hanbit Nuclear Power Plant 3 and the IBS Research Solution Center (RSC) for providing high performance computing resources. This work is supported by the Institute for Basic Science (IBS) under Project Code IBS-R016-A1 and the National Research Foundation (NRF) grant funded by the Korean government (MSIT) (NRF-2021R1A2C1013761 and NRF-2021R1A2C3010989), Republic of Korea. G. K. and J. N.

are supported by Fermi Research Alliance, LLC under Contract No. DEAC02-07CH11359 with the U.S. Department of Energy and the Kavli Institute for Cosmological Physics at the University of Chicago through an endowment from the Kavli Foundation and its founder Fred Kavli. D. K. is supported in part by the U.S. Department of Energy Grant No. DE-SC0010813.

Data availability—The scripts used to generate the figures in the main text are available at [77].

- [1] R. D. Peccei and H. R. Quinn, CP conservation in the presence of instantons, Phys. Rev. Lett. **38**, 1440 (1977).
- [2] F. Wilczek, Problem of strong P and T invariance in the presence of instantons, Phys. Rev. Lett. 40, 279 (1978).
- [3] S. Weinberg, A new light boson?, Phys. Rev. Lett. **40**, 223 (1978).
- [4] J. E. Kim, Weak interaction singlet and strong CP invariance, Phys. Rev. Lett. **43**, 103 (1979).
- [5] M. A. Shifman, A. I. Vainshtein, and V. I. Zakharov, Can confinement ensure natural CP invariance of strong interactions?, Nucl. Phys. B166, 493 (1980).
- [6] J. Preskill, M. B. Wise, and F. Wilczek, Cosmology of the invisible axion, Phys. Lett. 120B, 127 (1983).
- [7] L. F. Abbott and P. Sikivie, A cosmological bound on the invisible axion, Phys. Lett. **120B**, 133 (1983).
- [8] M. Dine and W. Fischler, The not so harmless axion, Phys. Lett. 120B, 137 (1983).
- [9] C. Bartram *et al.* (ADMX Collaboration), Search for invisible axion dark matter in the 3.3–4.2 μeV mass range, Phys. Rev. Lett. **127**, 261803 (2021).
- [10] K. M. Backes *et al.* (HAYSTAC Collaboration), A quantumenhanced search for dark matter axions, Nature (London) 590, 238 (2021).
- [11] O. Kwon *et al.* (CAPP Collaboration), First results from an axion haloscope at CAPP around 10.7 μeV, Phys. Rev. Lett. **126**, 191802 (2021).
- [12] R. L. Workman *et al.* (Particle Data Group Collaboration), Review of particle physics, Prog. Theor. Exp. Phys. 2022, 083C01 (2022).
- [13] E. Witten, Some properties of O(32) superstrings, Phys. Lett. **149B**, 351 (1984).
- [14] K. Choi, S. H. Im, and C. Sub Shin, Recent progress in the physics of axions and axion-like particles, Annu. Rev. Nucl. Part. Sci. 71, 225 (2021).
- [15] J. Jaeckel and A. Ringwald, The low-energy frontier of particle physics, Annu. Rev. Nucl. Part. Sci. 60, 405 (2010).
- [16] Y. K. Semertzidis and S. Youn, Axion dark matter: How to see it?, Sci. Adv. 8, abm9928 (2022).
- [17] J. Jaeckel and M. Spannowsky, Probing MeV to 90 GeV axion-like particles with LEP and LHC, Phys. Lett. B 753, 482 (2016).
- [18] Y. M. Andreev *et al.*, Improved exclusion limit for light dark matter from e+e- annihilation in NA64, Phys. Rev. D **104**, L091701 (2021).
- [19] F. Capozzi, B. Dutta, G. Gurung, W. Jang, I. M. Shoemaker, A. Thompson, and J. Yu, New constraints on ALP couplings

- to electrons and photons from ArgoNeuT and the Mini-BooNE beam dump, Phys. Rev. D **108**, 075019 (2023).
- [20] G. G. Raffelt, Astrophysical axion bounds, Lect. Notes Phys. 741, 51 (2008).
- [21] A. Caputo and G. Raffelt, Astrophysical axion bounds: The 2024 edition, Proc. Sci., COSMICWISPers (2024) 041.
- [22] V. Brdar, B. Dutta, W. Jang, D. Kim, I. M. Shoemaker, Z. Tabrizi, A. Thompson, and J. Yu, Axionlike particles at future neutrino experiments: Closing the cosmological triangle, Phys. Rev. Lett. 126, 201801 (2021).
- [23] G. Lucente, O. Straniero, P. Carenza, M. Giannotti, and A. Mirizzi, Constraining heavy axionlike particles by energy deposition in globular cluster stars, Phys. Rev. Lett. 129, 011101 (2022).
- [24] P. F. Depta, M. Hufnagel, and K. Schmidt-Hoberg, Updated BBN constraints on electromagnetic decays of MeV-scale particles, J. Cosmol. Astropart. Phys. 04 (2021) 011.
- [25] P. Carenza, O. Straniero, B. Döbrich, M. Giannotti, G. Lucente, and A. Mirizzi, Constraints on the coupling with photons of heavy axion-like-particles from globular clusters, Phys. Lett. B 809, 135709 (2020).
- [26] P. F. Depta, M. Hufnagel, and K. Schmidt-Hoberg, Robust cosmological constraints on axion-like particles, J. Cosmol. Astropart. Phys. 05 (2020) 009.
- [27] A. Caputo, G. Raffelt, and E. Vitagliano, Muonic boson limits: Supernova redux, Phys. Rev. D 105, 035022 (2022).
- [28] H. T. Janka, Neutrino-driven explosions, Handbook of Supernovae (Springer, Cham, 2017).
- [29] R. Bollig, W. DeRocco, P. W. Graham, and H.-T. Janka, Muons in supernovae: Implications for the axionmuon coupling, Phys. Rev. Lett. 125, 051104 (2020); 126, 189901(E) (2021).
- [30] R. Z. Ferreira, M. C. D. Marsh, and E. Müller, Strong supernovae bounds on ALPs from quantum loops, J. Cosmol. Astropart. Phys. 11 (2022) 057.
- [31] J. B. Dent, B. Dutta, D. Kim, S. Liao, R. Mahapatra, K. Sinha, and A. Thompson, New directions for axion searches via scattering at reactor neutrino experiments, Phys. Rev. Lett. **124**, 211804 (2020).
- [32] D. Aristizabal Sierra, V. De Romeri, L. J. Flores, and D. K. Papoulias, Axionlike particles searches in reactor experiments, J. High Energy Phys. 03 (2021) 294.
- [33] A. A. Aguilar-Arevalo *et al.* (CCM Collaboration), Prospects for detecting axionlike particles at the Coherent CAPTAIN-Mills experiment, Phys. Rev. D **107**, 095036 (2023).
- [34] S.-H. Seo *et al.*, Physics potential of a few kiloton scale neutrino detector at a deep underground lab in Korea, arXiv: 2309.13435.
- [35] H. M. Chang et al. (TEXONO Collaboration), Search of axions at the Kuo-Sheng nuclear power station with a highpurity germanium detector, Phys. Rev. D 75, 052004 (2007).
- [36] S. Sahoo, S. Verma, M. Mirzakhani, N. Mishra, A. Thompson, S. Maludze, R. Mahapatra, and M. Platt, Reactor-based search for axion-like particles using CsI(Tl) detector, arXiv:2407 14704.
- [37] J. J. Choi *et al.* (NEON Collaboration), Exploring coherent elastic neutrino-nucleus scattering using reactor electron antineutrinos in the NEON experiment, Eur. Phys. J. C **83**, 226 (2023).

- [38] J. J. Choi *et al.* (NEON Collaboration), Upgrade of the NaI(Tl) crystal encapsulation for the NEON experiment, J. Instrum. **19**, P10020 (2024).
- [39] G. Adhikari *et al.*, The COSINE-100 liquid scintillator veto system, Nucl. Instrum. Methods Phys. Res., Sect. A **1006**, 165431 (2021).
- [40] J. J. Choi, B. J. Park, C. Ha, K. W. Kim, S. K. Kim, Y. D. Kim, Y. J. Ko, H. S. Lee, S. H. Lee, and S. L. Olsen, Improving the light collection using a new NaI(Tl) crystal encapsulation, Nucl. Instrum. Methods Phys. Res., Sect. A 981, 164556 (2020).
- [41] G. Adhikari *et al.* (COSINE-100 Collaboration), The COSINE-100 data acquisition system, J. Instrum. 13, P09006 (2018).
- [42] G. H. Yu *et al.* (COSINE-100 Collaboration), Improved background modeling for dark matter search with COSINE-100, Eur. Phys. J. C **85**, 32 (2025).
- [43] S. M. Lee *et al.* (COSINE-100 Collaboration), Nonproportionality of NaI(Tl) scintillation detector for dark matter search experiments, Eur. Phys. J. C **84**, 484 (2024).
- [44] L. Swiderski, Response of doped alkali iodides measured with gamma-ray absorption and Compton electrons, Nucl. Instrum. Methods Phys. Res., Sect. A 705, 42 (2013).
- [45] G. Adhikari *et al.* (COSINE-100 Collaboration), Lowering the energy threshold in COSINE-100 dark matter searches, Astropart. Phys. **130**, 102581 (2021).
- [46] J. J. Choi et al. (NEON Collaboration), First direct search for light dark matter using the NEON experiment at a nuclear reactor, Phys. Rev. Lett. 134, 021802 (2025).
- [47] G. Adhikari *et al.* (COSINE-100 Collaboration), Background modeling for dark matter search with 1.7 years of COSINE-100 data, Eur. Phys. J. C **81**, 837 (2021).
- [48] E. Barbosa de Souza *et al.* (COSINE-100 Collaboration), Study of cosmogenic radionuclides in the COSINE-100 NaI (Tl) detectors, Astropart. Phys. **115**, 102390 (2020).
- [49] C. Ha *et al.*, Radon concentration variations at the Yangyang underground laboratory, Front. Phys. **10**, 1030024 (2022).
- [50] See Supplemental Material at http://link.aps.org/supplemental/10.1103/PhysRevLett.134.201002 for time dependent background model, which includes Refs. [37,38,42,48,49,51–54] and ALP signal generation, which includes Refs. [31,32,55–62].
- [51] J. Amaré, S. Cebrián, C. Cuesta, E. García, C. Ginestra, M. Martínez, M. Oliván, Y. Ortigoza, A. O. de Solórzano, C. Pobes, J. Puimedón, M. Sarsa, J. Villar, and P. Villar, Cosmogenic radionuclide production in NaI(Tl) crystals, J. Cosmol. Astropart. Phys. 02 (2015) 046.
- [52] P. Villar, J. Amaré, S. Cebrián, I. Coarasa, E. García, M. Martínez, M. A. Oliván, Y. Ortigoza, A. Ortiz de Solórzano, J. Puimedón, M. L. Sarsa, and J. A. Villar, Study of the cosmogenic activation in NaI(Tl) crystals within the anais experiment, Int. J. Mod. Phys. A 33, 1843006 (2018).
- [53] X. Li, B. Zheng, Y. Wang, and X. Wang, A study of daily and seasonal variations of radon concentrations in underground buildings, Journal of Environmental Radioactivity 87, 101 (2006).
- [54] Y. J. Ko *et al.* (NEOS Collaboration), Sterile neutrino search at the NEOS experiment, Phys. Rev. Lett. **118**, 121802 (2017).

- [55] M. Roos, Sources of gamma radiation in a reactor core, J. Nucl. Energy Part B React. Technol. 1, 98 (1959).
- [56] H. Bechteler, H. Faissner, R. Yogeshwar, and H. Seyfarth, The spectrum of  $\gamma$  radiation emitted in the FRJ-1 (Merlin) reactor core and moderator region, 1984. Juel-Spez–255.
- [57] H. Primakoff, Photo-production of neutral mesons in nuclear electric fields and the mean life of the neutral meson, Phys. Rev. **81**, 899 (1951).
- [58] A. Arvanitaki, S. Dimopoulos, S. Dubovsky, N. Kaloper, and J. March-Russell, String axiverse, Phys. Rev. D 81, 123530 (2010).
- [59] M. Cicoli, M. D. Goodsell, and A. Ringwald, The type IIB string axiverse and its low-energy phenomenology, J. High Energy Phys. 10 (2012) 146.
- [60] Xcom: Photon cross sections database, https://www.nist.gov/pml/xcom-photon-cross-sections-database. Accessed: 2024-12-09.
- [61] F. T. Avignone III, R. L. Brodzinski, S. Dimopoulos, G. D. Starkman, A. K. Drukier, D. N. Spergel, G. Gelmini, and B. W. Lynn, Laboratory limits on solar axions from an ultralow background germanium spectrometer, Phys. Rev. D 35, 2752 (1987).
- [62] G. Bellini et al., Search for solar axions emitted in the M1-transition of 7Li\* with Borexino CTF, Eur. Phys. J. C 54, 61 (2008).
- [63] G. Adhikari et al. (COSINE-100 Collaboration), Search for boosted dark matter in COSINE-100, Phys. Rev. Lett. 131, 201802 (2023).
- [64] J. Blumlein *et al.*, Limits on the mass of light (pseudo)scalar particles from Bethe-Heitler e + e and mu + mu pair production in a proton—iron beam dump experiment, Int. J. Mod. Phys. A **07**, 3835 (1992).
- [65] J. D. Bjorken, S. Ecklund, W. R. Nelson, A. Abashian, C. Church, B. Lu, L. W. Mo, T. A. Nunamaker, and P. Rassmann, Search for neutral metastable penetrating particles produced in the SLAC beam dump, Phys. Rev. D 38, 3375 (1988).
- [66] D. J. Bechis, T. W. Dombeck, R. W. Ellsworth, E. V. Sager, P. H. Steinberg, L. J. Teig, J. K. Yoh, and R. L. Weitz, Search

- for axion production in low-energy electron bremsstrahlung, Phys. Rev. Lett. **42**, 1511 (1979); **43**, 90(E) (1979).
- [67] E. M. Riordan *et al.*, A search for short lived axions in an electron beam dump experiment, Phys. Rev. Lett. **59**, 755 (1987).
- [68] A. Payez, C. Evoli, T. Fischer, M. Giannotti, A. Mirizzi, and A. Ringwald, Revisiting the SN1987A gamma-ray limit on ultralight axion-like particles, J. Cosmol. Astropart. Phys. 02 (2015) 006.
- [69] J. Jaeckel, P. C. Malta, and J. Redondo, Decay photons from the axionlike particles burst of type II supernovae, Phys. Rev. D 98, 055032 (2018).
- [70] G. Lucente and P. Carenza, Supernova bound on axionlike particles coupled with electrons, Phys. Rev. D 104, 103007 (2021).
- [71] M. J. Dolan, T. Ferber, C. Hearty, F. Kahlhoefer, and K. Schmidt-Hoberg, Revised constraints and Belle II sensitivity for visible and invisible axion-like particles, J. High Energy Phys. 12 (2017) 094; 03 (2021) 190(E).
- [72] E. Hardy and R. Lasenby, Stellar cooling bounds on new light particles: Plasma mixing effects, J. High Energy Phys. 02 (2017) 033.
- [73] S. N. Gninenko, D. V. Kirpichnikov, M. M. Kirsanov, and N. V. Krasnikov, The exact tree-level calculation of the dark photon production in high-energy electron scattering at the CERN SPS, Phys. Lett. B 782, 406 (2018).
- [74] L. Di Luzio, M. Giannotti, E. Nardi, and L. Visinelli, The landscape of QCD axion models, Phys. Rep. 870, 1 (2020).
- [75] J.-F. Fortin, H.-K. Guo, S. P. Harris, D. Kim, K. Sinha, and C. Sun, Axions: From magnetars and neutron star mergers to beam dumps and BECs, Int. J. Mod. Phys. D 30, 2130002 (2021).
- [76] B. Batell *et al.*, Dark sector studies with neutrino beams, in *Snowmass 2021* (2022), 7, arXiv:2207.06898.
- [77] H. S. Lee, ROOT Scripts for Figures in "New Constraints on Axion-Like Particles with the NEON Detector at a Nuclear Reactor", 10.5281/zenodo.15220206.